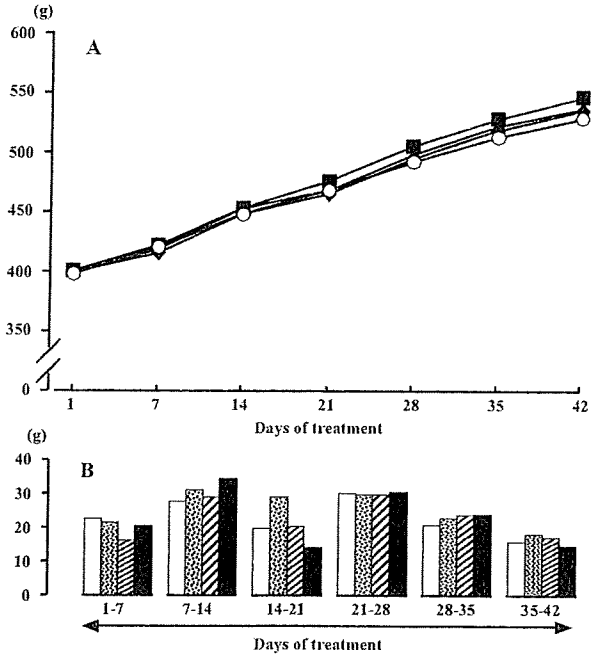

Fig. 3. Changes in body weight (A) and its gain (B) in male rats treated orally with 4-methylbenzoic acid for 42-days at dose level of 0 (○ and open column), 100 (■ and dashed column), 300 (▲ and hatched column) or 1,000 mg/kg/day (♦ and closed column) in the reproduction/developmental toxicity screening test. Each value represents the average for 13 animals.

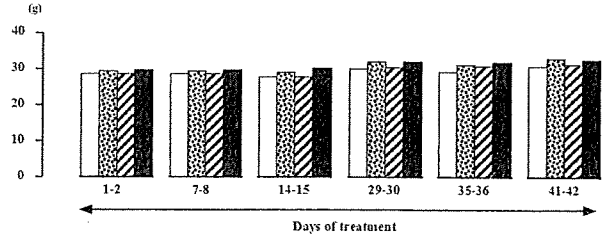

Fig. 4. Changes in food consumption of male rats treated orally with 4-methylbenzoic acid for 42-days at dose level of 0 (open column), 100 (dashed column), 300 (hatched column) or 1,000 mg/kg/day (closed column) in the reproduction/developmental toxicity screening test. Each column represents the average for 13 males.

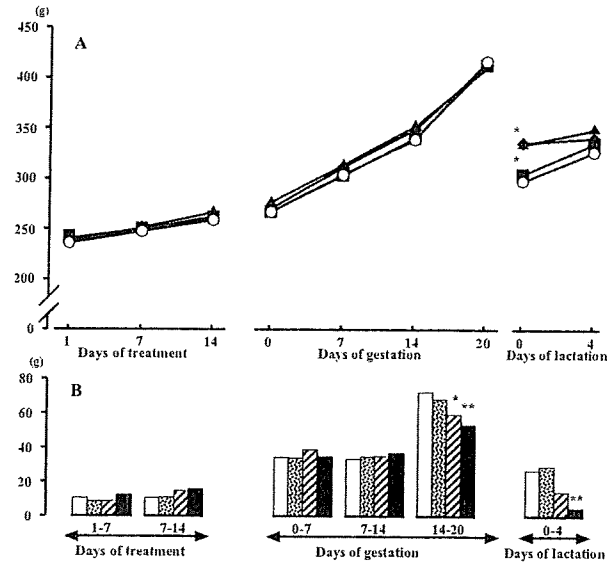

Fig. 5. Changes in body weight (A) and its gain (B) in female rats treated orally with 4-methylbenzoic acid at a dose level of 0 (○ and open column), 100 (■ and dashed column), 300 (▲ and hatched column) or 1,000 mg/kg/day (♦ and closed column) in the reproduction/developmental toxicity screening test. Administration of the compound was started 2 weeks prior to mating, and was continued through mating period and gestation period until 3 days after delivery. Each value during the pre-mating treatment period represents the average for 13 animals. That during the gestation and lactation periods represents the average for 9-13 dams. * and ** indicate significant difference from control at $p < 0.05$ and 0.01, respectively.

control. Males in the groups given 300 mg/kg or less did not show such abnormalities at any part of their epididymis (Table 6). In the testis, no abnormal findings related to the doses of the compound were observed.

Reproductive performances in the reproduction/developmental study

Except one female in the control and one female in the 100 mg/kg treated groups, all the females revolved on a regular 4-day estrous cycle until mating (data not shown). Mating performance and dam data are shown in Table 7. None of indices for mating performance were different between the compound treated group and the control group. In addition, the number of corpora lutea, which represented the number of oocytes shed for impregnation, was not different between these groups. Thus, the compound did not affect the estrous cycle, ovulation or mating, at any dose level.

Although all of the females that had copulated in the 100 mg/kg and less treated groups became pregnant, one such female and four such females in the 300 mg/kg and 1,000 mg/kg treated groups, respectively, did not become pregnant (Table 7). The Fisher's direct probability test indicated that there was a significant difference in the fertility between the control and the 1,000 mg/kg treated groups, which indicated that the compound disrupted fertility at 1,000 mg/kg.

As shown in Table 7, pregnant females delivered live fetuses without differences in gestation length between the control and the compound treated groups. However, the implantation index and the number of pups born were significantly decreased in the 300 mg/kg or more treated groups. Furthermore, the numbers of pups alive on Days 0 and 4 of lactation were significantly smaller in the 1,000 mg/kg treated group than those in the control. The other dam data, such as the birth index, the live birth index and the viability index on Day 4 of lactation, were not affected by the treatment. In addition, pup body weights at birth and on Day 4 of lactation and the sex ratios on these days were not affected by the treatment, in any group.

At necropsy of females, the uterus of the female that failed to become pregnant in the 300 mg/kg treated group showed ballooning and accumulation of cloudy fluid. Histopathology of the uterus revealed lumen dilatation and cellular infiltration of neutrophils in the epithelium and endometrial stroma, with edema in the endometrial stroma. In the 1,000 mg/kg treated group, however, no abnormality was observed in the reproductive organs of the four females that failed to become pregnant, either, at the gross necropsy or in the histopathological examination of the ovary, while a moderate increase in atretic follicles was observed in one of the females. Including this case, there were no histopathological findings in the ovary related to doses of the compound (data not shown).

No abnormalities in the morphology or behavior of pups was noted in any group, except the following occasional cases in a single dam of the 1,000 mg/kg treated group: temporary cyanosis at birth and dilatation of renal pelvis at necropsy on Day 4 of lactation in one male pup.

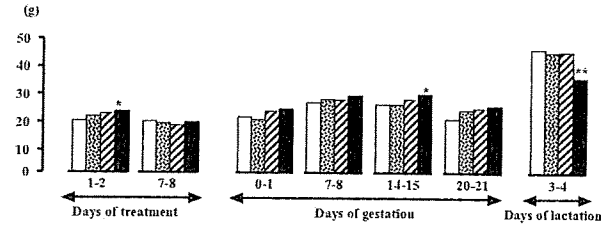

Fig. 6. Changes in food consumption of female rats treated orally with 4-methylbenzoic acid at dose levels of 0 (open column), 100 (dashed column), 300 (hatched column) or 1,000 mg/kg/day (closed column) in the reproduction/developmental toxicity screening test. Administration of the compound was started 2 weeks prior to mating, and was continued through mating period and gestation period until 3 days after delivery. Each value during the pre-mating treatment period represents the average for 13 females. That during the gestation and lactation periods represents the average for 9-13 dams. * and ** indicate significant difference from control at $p < 0.05$ and 0.01, respectively.

Table 5. Weights of testes and epididymides in rats treated orally with 4-methylbenzoic acid for 42-days in reproduction/developmental toxicity screening test

Dose (mg/kg)	0	100	300	1,000
Number of animals	13	13	13	13
Body weight (g)	527.9 ± 37.8	549.9 ± 42.8	541.6 ± 26.6	542.4 ± 30.7
Absolute weight				
Testes (g)	3.37 ± 0.24	3.29 ± 0.19	3.29 ± 0.22	3.31 ± 0.17
Epididymides (g)	1.28 ± 0.08	1.27 ± 0.08	1.24 ± 0.07	1.13 ± 0.09**
Relative weight (g/100 g)				
Testes	0.64 ± 0.07	0.60 ± 0.06	0.61 ± 0.04	0.61 ± 0.05
Epididymides	0.24 ± 0.03	0.23 ± 0.02	0.23 ± 0.01	0.21 ± 0.02**

Values represent average ± S.D.
**, significant difference from control at $p < 0.01$.

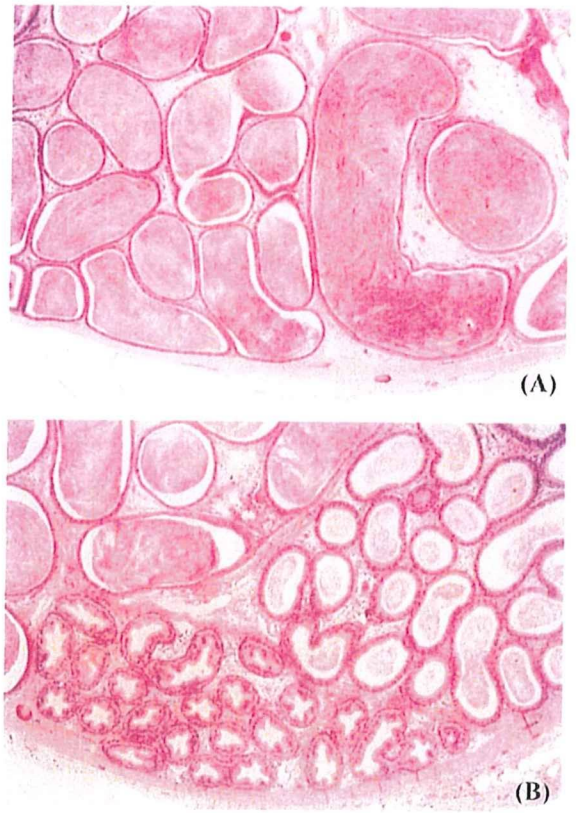

Fig. 7. Representative photographs of microscopic cross section of the cauda epididymis in male rats treated orally with 4-methylbenzoic acid at dose levels of 0 (A) or 1,000 mg/kg/day (B) in the reproduction study conducted under the OECD test guideline 421. Note that a few sperm are found in the lumen of the compound treated rats (B), and the epithelial height of the lumen becomes high. In contrast, the epithelial height of the lumen in the vehicle treated rats (A) becomes low by filling sperm in the lumen. Hematoxylin-eosin stain, x36.

DISCUSSION

Although the results obtained from the present studies are limited to short-term oral toxicity of 4-methylbenzoic acid, they indicate some toxicological properties of the compound. Namely, inconsistent effects of the compound on the epididymis indicate different toxicological potencies of the compound in male animals between the 28-day study and the reproduction/developmental study. While oral daily administration with 1,000 mg/kg of the compound reduced epididymal weight and caused oligo/azoospermia in the cauda epididymal lumen in the reproduction/developmental study, the same dose of the compound did not cause such effects in the 28-day study. Thus, the compound exerts adverse effects only on adult males when given for 42 days. Except that, repeated administration of 1,000 mg/kg of the compound led to similar results in males in both studies, such as a temporary salivation after dosing and no effects on body weight increase or food consumption. Therefore, the inconsistencies may be caused by differences in the timing or duration of administration.

The oligo/azoospermia seemed to develop at the distal part of the epididymis, since no abnormalities were observed in the caput epididymis and since there were normal lumens in the cauda epididymis. As reported by Robaire *et al.* (2006), spermatozoa enter the epididymis with testicular fluid and progress downward toward the vas deferens by smooth muscle contraction. In the reproduction/developmental study, the oligo/azoospermia developed where mature spermatozoa are stored. Spermatozoa are found in seminiferous tubules at the time of puberty, approximately 6 weeks of age in the rat, and it takes at least 10 or 15 days to reach the cauda epididymis (Sommer *et al.*, 1996; Robaire *et al.*, 2006). We have confirmed previously that spermatozoa are found in the cauda epididymis at 56 days of age at the youngest in the Sprague-Dawley derived inbred rats, which attain puberty at a comparable range of ages to Sprague-Dawley rats (Sato *et al.*, 2002). Since the compound was administered for 4 weeks in the 28-day study, from 5 weeks of age, the compound could influence epididymal spermatozoa for a short period. The storage period of spermatozoa in the cauda epididymis is estimated to be one week. In contrast, the compound was administered from 10 weeks of age in the reproduction/developmental study and could influence spermatozoa in all segments of the epididymis for 42 days. The inconsistent adverse effects of the compound on the cauda epididymis between the studies could be explained by either, the timing or the duration, of the administration.

Although the results obtained from the reproduction/developmental study seemed to suggest epididymal spermatozoa as the toxicological target of the compound, 4-methylbenzoic acid could influence spermatozoa function during their transit to the cauda epididymis. It has been reported that spermatozoa become functionally mature during transit to the distal part of the epididymis, while they are protected from oxidative stress and harmful xenobiotics by the blood-epididymis barrier and different types of antioxidant enzymes in each segment of the epididymis (Tengpwski *et al.*, 2007; Kim *et al.*, 2004; Robaire *et al.*, 2006). Therefore, detailed investigation of the effects of the compound on production, function and transition of spermatozoa is required.

Table 6. Histopathological findings of testis and epididymis in rats treated orally with 4-methylbenzoic acid for 42 days in the reproduction/ developmental toxicity screening test

Dose	0 mg/kg					100 mg/kg					300 mg/kg					1,000 mg/kg				
Grade	-	±	+	++	+++	-	±	+	++	+++	-	±	+	++	+++	-	±	+	++	+++
Testis	(13)					(13)					(13)					(13)				
Atrophy, focal, seminiferous tubule, bilateral	12	1	0	0	0	12	1	0	0	0	13	0	0	0	0	13	0	0	0	0
Multinucleated giant cell, seminiferous tubule	13	0	0	0	0	13	0	0	0	0	13	0	0	0	0	12	1	0	0	0
Epididymis	(13)					(13)					(13)					(13)				
A few number of sperm, lumen, cauda, bilateral	13	0	0	0	0	13	0	0	0	0	13	0	0	0	0	**0	11	2	0	0
																		##		
Cell debris, lumen, cauda, bilateral	12	1	0	0	0	13	0	0	0	0	13	0	0	0	0	8	5	0	0	0
Spermatid granuloma, cauda, unilateral	13	0	0	0	0	13	0	0	0	0	12	0	1	0	0	13	0	0	0	0

-, Negative; ±, Very slight; +, Slight; ++, Moderate; +++, Severe

** and ##, significant difference from control at $p < 0.01$ for incidence and grades of the findings, respectively.

Table 7. Mating performances and dam data of rats treated orally with 4-methylbenzoic acid in the reproduction/developmental toxicity screening test

Dose (mg/kg)	0	100	300	1,000
Mating performance				
Copulated pairs/Co-housed pairs (%)	13/13 (100)	13/13 (100)	12/13 (92.3)	13/13 (100)
Pregnant females/Copulated pairs (%)	13/13 (100)	13/13 (100)	11/12 (91.7)	9/13 (69.2)*
Pairing days until copulation [a]	3.0 ± 3.4	2.4 ± 1.3	2.4 ± 1.3	3.2 ± 3.3
Number of estrus revolved until copulation [a]	1.0 ± 0.0	1.0 ± 0.0	1.0 ± 0.0	1.1 ± 0.3
Dam data				
Number of pregnant females with live pups	13	13	11	9
Gestation length in days [a]	22.3 ± 0.5	22.5 ± 0.5	22.3 ± 0.5	22.8 ± 0.4
Number of corpora lutea [a]	16.2 ± 1.3	15.7 ± 1.3	16.2 ± 1.5	15.9 ± 1.3
Number of implantation sites [a]	16.0 ± 1.3	15.4 ± 1.0	14.0 ± 2.4	12.1 ± 5.3
Implantation index [a, b]	99.1 ± 2.2	98.2 ± 3.5	86.5 ± 12.6**	75.9 ± 32.6*
Day 0 of lactation				
Number of pups born [a]	15.2 ± 1.4	14.1 ± 1.8	12.5 ± 2.1**	10.2 ± 5.1**
Delivery index [a, c]	94.7 ± 5.2	91.4 ± 8.5	90.1 ± 8.4	82.9 ± 19.5
Number of pups alive	14.3 ± 1.7	14.1 ± 1.8	12.3 ± 2.2	10.0 ± 5.0*
Birth index [a, d]	89.7 ± 10.4	91.4 ± 8.5	88.0 ± 9.1	81.5 ± 19.8
Live birth index [a, e]	94.8 ± 10.5	100 ± 0	97.6 ± 4.2	98.2 ± 3.7
Sex ratio [a, f]	54.1 ± 14.3	51.9 ± 12.8	46.6 ± 13.8	59.8 ± 17.7
Day 4 of lactation				
Number of pups alive [a]	14.3 ± 1.7	13.9 ± 1.8	12.3 ± 2.2	9.7 ± 5.3*
Viability index [a]	100 ± 0	99.0 ± 3.7	100 ± 0	88.1 ± 33.1
Sex ratio [a, f]	54.1 ± 14.3	52.3 ± 12.3	46.6 ± 13.8	54.4 ± 9.5
Pups weight on Day 0 of lactation (g/pup)				
Male [a]	6.8 ± 0.4	7.0 ± 0.5	7.0 ± 0.5	6.7 ± 0.3
Female [a]	6.5 ± 0.4	6.7 ± 0.6	6.6 ± 0.5	6.4 ± 0.5
Pups weight on Day 4 of lactation (g/pup)				
Male [a]	10.7 ± 1.0	11.2 ± 1.1	11.8 ± 1.2	11.1 ± 0.9
Female [a]	10.3 ± 1.0	10.7 ± 1.1	11.2 ± 1.3	10.5 ± 0.9

[a] Average ± S.D.; [b] (Number of implantation sites/Number of corpora lutea) × 100, %; [c] (Number of pups born/Number of implantation sites) × 100, %; [d] (Number of live pups on Day 0 of lactation/Number of implantation sites) × 100, %; [e] (Number of live pups on Day 0 of lactation/Number of pups born) × 100, %; [f] (Number of live male pups/Number of live pups) × 100, %
* and **, significant difference from control at $p < 0.05$ and 0.01, respectively.

The reproduction/developmental study revealed that the compound reduced fertility of animals within a relatively short period of dosing, since the four males that failed to impregnate in the 1,000 mg/kg treated group had copulated on Days 16, 19, 19 and 28 of treatment. Furthermore, the compound increased preimplantation loss and decreased implantation index at a lower dose level than that caused oligo/azoospermia. It is not clear whether the reduced fertility and the increase in the preimplantation loss are consequent effects of the compound on the epididymal spermatozoa or are effects on such as fertilization, early embryonic development or implantation, although the results obtained from the reproduction/developmental study indicate no adverse effects on female reproductive function until mating.

Because mating was done within the same dose groups

in the reproduction/developmental study, it was impossible to determine the target sex of the compound. The reproductive toxicities of several compounds related to 4-methylbenzoic acid have been studied. A feeding administration of *p*-nitrobenzoic acid (CAS No. 62-23-7) (NTP, 1994) and m-nitrobenzoic acid (CAS No. 121-92-6) has been found to reduce the number of offspring in continuous breeding studies in CD-1 mice (NTP/NIEHS, 1997). Crossover mating conducted in these studies revealed that female reproduction is more sensitive than male reproduction. On the other hand, 3-methylbenzoic acid (CAS No. 99-04-7) and 4-hydroxybenzoic acid (CAS No. 99-96-7) did not show any reproductive toxicity in studies conducted under a protocol similar to the reproduction/developmental study (Nagao *et al.*, 1997; Yamamoto *et al.*, 1999), although estrogenic potency of 4-hydroxybenzoic acid was observed in a uterotrophic assay (Lemini *et al.*, 1997). Detailed investigation, such as crossover mating, quantification and qualification of spermatozoa, may elucidate the characteristics of the reproductive toxicity of 4-methylbenzoic acid.

In the reproduction/developmental study, maternal body weight was reduced during the latter period of gestation at the dose levels of 300 mg/kg or more, whereas it did not affect female body weight, at any dose level, in the 28-day study. It is clear, however, that the decrease in the maternal body weight was not caused by the direct toxicity of the compound. It was caused by a small litter size resulting from a reduced number of implantations, as discussed above, since fetal weight in the uterus greatly contributes to maternal body weight during the latter period of gestation. Comparable or greater food consumption during this period and greater body weight after parturition in dams of these groups also indicate no adverse effects of the compound on the maternal animals. Decreases in food consumption and body weight gain during the lactation period in the 1,000 mg/kg treated group might be physiological changes due to a smaller demand of nutrition for the small litter size.

In the males, urine specific gravity was decreased in the 300 mg/kg or more treated groups. The change, however, was reflected the increase in urine volume due to increased water consumption, and did not accompany morphological alterations or functional impairments of their kidneys. Therefore, the change was judged as a physiological response. Except for the effects on the epididymis in the reproduction/development study, no systemic effect of the compounds was observed in the males of both studies.

In the females, a slight increase in food consumption was observed in the 1,000 mg/kg treated group at the beginning of dosing in both studies. In the 28-day study, increase in AST activity and decrease in serum total protein concentration were observed in the 1,000 mg/kg treated females. Since increase in AST activity has been reported as an effect of 3-methylbenzoic acid (CAS No. 99-04-7) in the study noted above (Yamamoto *et al.*, 1999), 4-methylbenzoic acid may slightly alter female AST activity. Thus, the compound affected females at the dose level of 1,000 mg/kg. However, all these changes did not accompany structural changes and changes in organ weights. Therefore, repeated dosing of the compound may affect females at the dose level of 1,000 mg/kg, but may not affect adversely, at any dose level.

From these results, the no-observed-effect-level (NOEL) for reproductive toxicity is considered to be 100 mg/kg, whereas 1,000 mg/kg did not show any effect on neonates. That for repeated dose toxicity is considered to be 300 mg/kg for male and female rats in the both studies, but toxic effects on the epididymis differed between the studies. Thus, 4-methylbenzoic acid has a potential for reproductive toxicity and deserves further study, taking the exposure state into consideration, as discussed above, since it has been reported that the reproduction/developmental study provides screening information but does not provide a complete characterization and evaluation of reproductive or developmental toxicity (Gelbke *et al.*, 2004).

ACNOWLEDGMENT

This study was partially supported by the Ministry of Health, Labour and Welfare as a part of programs of safety examination for existing chemical substances.

REFERENCES

Gelbke, H.P., Fleig, H., Meder, M. and German Chemical Industry Association. (2004): SIDS reprotoxicity screening test update: testing strategies and use. Regul. Toxicol. Pharmacol., **39**, 81-86.

Kim, E., Nishimura, H., Iwase, S., Yamagata, K., Kashiwabara, S. and Baba, T. (2004): Synthesis, processing, and subcellular localization of mouse ADAM3 during spermatogenesis and epididymal sperm transport. J. Reprod. Dev. **50**, 571-578.

Lemini, C., Silva, G., Timossi, C., Luque, D., Valverde, A., González-Martínez, M., Hernández, A., Rubio-Póo, C., Chávez Lara, B. and Valenzuela F. (1997): Estrogenic effects of p-hydroxybenzoic acid in CD1 mice. Environ. Res., **75**, 130-134.

Mineshita, T., Toteno, I., Yui, Y., Furukawa, S. and Wakabayashi, K. (1978): Acute toxicity study of p-toluic acid, The Clinical Report, **12**, 1893-1904.

Nagao, T., Kuwagata, M., Kato, H. and Miyahara, T. (1997): Combined repeat dose and reproductive/developmental toxicity

screening test of hydroxybenzoic acid in rats. Toxicity Testing Reports of Environmental Chemicals **5**, 251-257.

National Toxicology Program (1994): NTP Toxicology and Carcinogenesis Studies of p-Nitrobenzoic Acid (CAS No. 62-23-7) in F344/N Rats and B6C3F1 Mice (Feed Studies). Natl. Toxicol. Program Tech. Rep. Ser. **442**,1-306.

National Toxicology Program / National Institute of Environmental Health Sciences (1997): Reproductive toxicology. m-Nitrobenzoic acid. Environ. Health Perspect., **105** (Suppl. 1), 325–326.

OECD (1997a): OECD Guideline for the Testing of Chemicals 407, "Repeated Dose 28-day Oral Toxicity Study in Rodents" adopted on 27 July 1995.

OECD (1997b): OECD Guideline for the Testing of Chemicals 421, "Reproduction/Developmental Toxicity Screening Test" adopted on 27 July 1995.

OECD (2004): The 2004 OECD list of high production volume chemicals.

Robaire, B., Hinton, B. T. and Orgebin-Crist, M-C. (2006); The epididymis. In Knobil and Neill's Physiology of Reproduction, 3rd ed. (Neill, J. D. ed.) pp.1071-1148, Academic Press, USA and UK.

Sato, M., Ohta, R., Kojima, K., Shirota, M., Koibuchi, H., Asai, S., Watanabe, G. and Taya, K. (2002): A comparative study of puberty and plasma gonadotropin and testicular hormone levels in two inbred strains of Hatano rats. J. Reprod. Dev., **48**, 111-119.

Sommer, R. J., Ippolito, D. L., and Peterson, R.E.(1996): In utero and lactational exposure of the male Holtzman rat to 2,3,7,8-tetrachlorodibenzo-p-dioxin: decreased epididymal and ejaculated sperm numbers without alterations in sperm transit rate. Toxicol. Appl. Pharmacol., **140**, 146-153.

Tengowski, M.W., Feng, D., Sutovsky, M. and Sutovsky, P. (2007); Differential expression of genes encoding constitutive and inducible 20S proteasomal core subunits in the testis and epididymis of theophylline- or 1,3-dinitrobenzene-exposed rats. Biol. Reprod., **76**,149-163.

Yamamoto, Y., Ito, Y., Nosa, A., Ito, M., Akagi, H. and Hoshi, F. (1999): Combined repeat dose and reproductive/developmental toxicity screening test of 3-methylbenzoic acid in rats. Toxicity Testing Reports of Environmental Chemicals **7**, 302-308.

NANOS2 interacts with the CCR4-NOT deadenylation complex and leads to suppression of specific RNAs

Atsushi Suzuki[a], Katsuhide Igarashi[b], Ken-ichi Aisaki[b], Jun Kanno[b], and Yumiko Saga[c,1]

[a]Interdisciplinary Research Center, Yokohama National University, Yokohama, Kanagawa 240-8501, Japan; [b]Cellular and Molecular Toxicology Division, National Institute of Health Sciences, Setagayaku, Tokyo 158-8501, Japan; and [c]Division of Mammalian Development, National Institute of Genetics, Mishima 411-8540, Japan

Edited by Ruth Lehmann, New York University Medical Center, New York, NY, and approved December 30, 2009 (received for review August 2, 2009)

Nanos is one of the evolutionarily conserved proteins implicated in germ cell development. We have previously shown that NANOS2 plays an important role in both the maintenance and sexual development of germ cells. However, the molecular mechanisms underlying these events have remained elusive. In our present study, we found that NANOS2 localizes to the P-bodies, known centers of RNA degradation that are abundantly accumulated in male gonocytes. We further identified by immunoprecipitation that the components of the CCR4-NOT deadenylation complex are NANOS2-interacting proteins and found that NANOS2 promotes the localization of CNOT proteins to P-bodies in vivo. We also elucidated that the NANOS2/CCR4-NOT complex has deadenylase activity in vitro, and that some of the RNAs implicated in meiosis interact with NANOS2 and are accumulated in its absence. Our current data thus indicate that the expression of these RNA molecules is normally suppressed via a NANOS2-mediated mechanism. We propose from our current findings that NANOS2-interacting RNAs may be recruited to P-bodies and degraded by the enzymes contained therein through NANOS2-mediated deadenylation.

germ cells | P-body | meiosis

In the mouse, the primordial germ cells (PGCs) are segregated from the somatic cell lineage at an early gastrulation stage (1). Although the PGCs are potent producers of both oogonia and spermatogonia, sexual differentiation is induced after their colonization of the embryonic gonads with somatic cells. However, the initial steps leading to diversification of these cells have long remained unsolved. Retinoic acid (RA) signaling has recently been identified as the initial trigger for feminization (2). RA molecules derived from the mesonephros trigger meiotic initiation in female gonocytes via the induction of the RA responsive gene *Stra8*, which is required for premeiotic replication (3). In contrast, male gonocytes are protected from exposure to RA by CYP26B1, an RA metabolizing enzyme produced from somatic cells, resulting in the suppression of meiosis up to E13.5 (4, 5). In addition, *Nanos2* expression begins after E13.5 and is required for the maintenance and promotion of the male germ cell state (6).

Nanos is an evolutionarily conserved RNA-binding protein that is essential for germ cell development (7). In *Drosophila*, Nanos forms a complex with another RNA-binding protein, Pumilio, and represses the translation of the *hunchback*, *cyclin B*, and *hid* mRNAs thereby establishing embryonic polarity, mitotic quiescence, and suppression of apoptosis, respectively (8–10). Three *Nanos* homologs, *Nanos1–3*, exist in the mouse, among which *Nanos3* and *Nanos2* are expressed in the germ cells and are required to protect these cells from undergoing apoptosis during migration and after colonization of the male gonads, respectively (11, 12). In addition, *Nanos2* plays a key role during the sexual development of germ cells by suppressing meiosis and promoting male-type differentiation in the embryonic male gonads. Moreover, the forced expression of *Nanos2* in female gonocytes can induce the suppression of meiosis and promotion of male-type gene expression (6). However, the molecular mechanisms underlying how this protein accomplishes such pleiotropic functions in the mouse germ cells remain unknown.

In our present study, we find that NANOS2 localizes to P-bodies, a central hub of RNA degradation (13, 14). We further identify components of the CCR4-NOT deadenylation complex as NANOS2-associated proteins in vivo, which can cleave poly(A) RNA in vitro. We also show that specific mRNAs interact with NANOS2, and thus propose that NANOS2 plays a role in recruiting the CCR4-NOT deadenylation complex to trigger the degradation of specific RNAs.

Results

NANOS2 Localizes at P-Bodies During Gonocyte Development. To increase our understanding of the molecular mechanisms underlying the function of the NANOS2 protein, we first analyzed the cellular localization of this protein by immunostaining. Consistent with the results of our previous western analyses (15), NANOS2 protein was first detectable at E13.5 in the cytoplasm of male mouse gonocytes. This signal intensity increased until about E16.5 and then slightly decreased by E17.5. In addition, we found that some of the NANOS2 proteins formed discrete foci, the number of which gradually increased until E16.5 and then decreased thereafter (Fig. S1 *A–F*). Because *Drosophila* Vasa and Tudor are known to form cytoplasmic foci (16, 17), which are the polar granules in the germ plasm, we speculated that these NANOS2 foci might colocalize with the mouse homologs of Vasa, MVH (mouse vasa homolog) (18) and the Tudor protein TDRD1 (tudor domain containing 1) (19). However, these foci did not show any clear colocalization with NANOS2 (Fig. S2 *A–F*). We next tested the possibility that the NANOS2 foci might correspond to P-bodies, which are known to function as a center of RNA degradation. We thus conducted double-immunostaining using antibodies against the P-body components DCP2 and XRN1, an mRNA decapping enzyme and RNA exonuclease, respectively (13, 14). We were initially surprised to find that many P-bodies could be specifically observed only in germ cells and not in the somatic cells in E15.5 male gonads, and also that the NANOS2 foci clearly merged with those of DCP2 and XRN1 (Fig. 1 *A–F*) from E13.5 to E17.5 (Fig. S3 *A–F*). This suggests the possibility that NANOS2 may be involved in RNA degradation.

Nanos2 Functions in the Formation of P-Bodies. We further examined the status of the P-bodies in the mouse gonads of both sexes by immunostaining of p54/RCK, a homolog of *Drosophila* Me31B and also a marker of these structures (20). Although the P-bodies seemed to be present in the same number and size in the gonocytes of both sexes at E12.5, they were gradually reduced and eventually lost by E14.5 in female gonocytes (Fig. S4 *E* and *F*). In contrast, the P-bodies become much larger in both number and

Author contributions: A.S. and Y.S. designed research; A.S., performed research; K.I., K.. A., and J.K. analyzed data of microarray analyses; and A.S. and Y.S. wrote the paper.

The authors declare no conflict of interest.

This article is a PNAS Direct Submission.

[1]To whom correspondence should be addressed. E-mail: ysaga@lab.nig.ac.jp.

This article contains supporting information online at www.pnas.org/cgi/content/full/0908664107/DCSupplemental.

www.pnas.org/cgi/doi/10.1073/pnas.0908664107

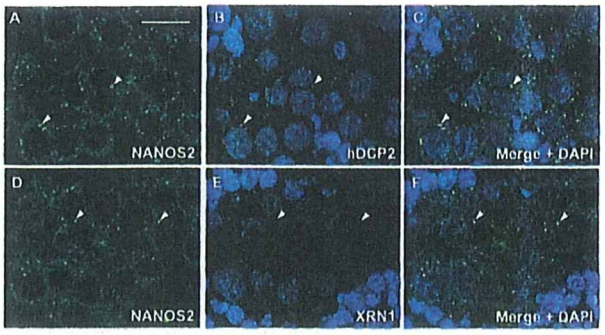

Fig. 1. NANOS2 localizes to the P-bodies in male mouse gonocytes. (*A–L*) Sections prepared from wild-type E15.5 male gonads were double-stained with mouse anti-NANOS2 (green) (*A* and *D*) and either hDCP2 (*B*) or mXRN1 (*E*) antibodies (red staining in each case). Arrowheads indicate colocalization of NANOS2 and hDCP2 (C) or XRN1 (*F*). DNA was counterstained with DAPI (blue). (Scale bar in *A*, 20 μm for all panels.)

size from E14.5, concomitant with the onset of NANOS2 expression, in male gonocytes (Fig. S4 *A–D*).

To further explore the role of NANOS2 in P-body formation, we examined the status of these structures in the absence of *Nanos2*. Although there were, somewhat unexpectedly, many P-bodies detected in both *Nanos2*$^{+/-}$ and *Nanos2*$^{-/-}$ male gonocytes at E13.5, their sizes became gradually larger, whereas their number became smaller, at the later stages of embryogenesis in the absence of *Nanos2* (Fig. 2 *A–D*). This was also observed in *Nanos2, Bax* double-null male gonocytes (Fig. 2 *E* and *F*), where apoptotic cell death was suppressed, suggesting that apoptosis does not affect P-body status. This indicates that NANOS2 is not essential for the assembly of P-bodies but is required for the maintenance of their normal state. To further elucidate the functions of NANOS2 in P-body formation, we also examined the status of the P-bodies in NANOS2-expressing female gonocytes (6). Although they could not be detected in normal female gonocytes at E16.5, we found many P-bodies in NANOS2-expressing female cells and additionally observed that NANOS2 localizes at the P-bodies in these cells (Fig. 2 *G–I*). These data indicate that NANOS2 is sufficient to maintain the number of P-bodies when female gonocytes have acquired a male-type phenotype due to NANOS2 expression.

NANOS2 Interacts with the CCR4-NOT Deadenylation Complex and Regulates Its Localization. To explore the molecular functions of NANOS2, we searched for proteins that interact with it. To this end, we prepared male gonadal extracts from *Nanos2*$^{+/-}$ and *Nanos2*$^{-/-}$ embryos at E14.5 and subjected them to immunoprecipitation with anti-NANOS2 antibodies. We found that two major bands of more than 200 kDa were exclusively precipitated from *Nanos2*$^{+/-}$ gonads, and by mass spectrometric analysis identified these products as CNOT1, a component of the CCR4-NOT deadenylation complex (13) (Fig. 3A).

In further immunoprecipitation experiments, we used a transgenic mouse line expressing a FLAG-tagged NANOS2 under the direct control of the *Nanos2* enhancer (15) (Fig. S5*A*), since we had confirmed that this fusion protein was functional (Fig. S5 *B–F*) and localized at the P-bodies (Fig. S5 *G–I*). Western analyses revealed that CNOT1 coprecipitates with FLAG-tagged NANOS2 (Fig. 3*B, Upper*), confirming the results of our mass spectrometric analysis. We also found that other components of the CCR4-NOT complex, CNOT3, CNOT6L/Ccr4b, CNOT7/Caf1a, and CNOT9/Rcd1 (13, 21), also coprecipitated with FLAG-tagged NANOS2, indicating that NANOS2 associates with the CCR4-NOT deadenylation complex in vivo. We additionally found that this interaction is independent of RNA, as the levels of coprecipitated CNOT proteins were not affected by treatments with RNase (Fig. 3*B*). Finally, these CNOT proteins were found to colocalize with NANOS2 in P-bodies (Fig. 3 *C–E* and Fig. S6 *A–I*), suggesting that this complex may play a role in the activities of these elements.

To better understand the physiological significance of its interaction with NANOS2, we investigated the localization of CCR4-NOT deadenylation complex in *Nanos2*$^{-/-}$ male gonads by immunostaining CNOT proteins with DCP1A, another decapping enzyme and also a component of P-bodies (13, 14). Although CNOT3 was found to clearly localize to P-bodies in *Nanos2*$^{+/-}$ male gonads (Fig. 3 *F–H*), we detected only weak signals for this protein in P-bodies in the absence of NANOS2 (Fig. 3 *I–K*) even though the levels of CNOT3 are not reduced in *Nanos2*$^{-/-}$ male gonads (Fig. 3*L*). We obtained similar results for CNOT1 (Fig. S7). These data suggest that NANOS2 promotes the localization of the CCR4-NOT deadenylation complex to P-bodies, although a subpopulation of this complex still remains in these structures in the absence of NANOS2, possibly via a NANOS2-independent mechanism. Based on these findings and the fact that the CCR4-NOT deadenylation complex regulates the first step of mRNA degradation (22), we speculate that NANOS2 recruits this deadenylation complex to P-bodies where it promotes the degradation of RNAs.

Complex of NANOS2 and CCR4-NOT Deadenylation Complex in Male Germ Cells Retains Deadenylase Activity. To address the critical question of whether NANOS2-interacting deadenylase actually has catalytic activity, we used NANOS2-overexpressing (NANOS2 O/E) adult testes to obtain sufficient amounts of this protein and thus overcome the limitations of using embryonic testis in biochemical analyses. In the testis of the postnatal mouse, NANOS2 is expressed in a small population of undifferentiated spermatogonia (23) and localizes to P-bodies (Fig. S8 *A–C*) as in the male gonocytes. This expression is subsequently lost as these cells differentiate. However, if FLAG-tagged NANOS2 is forcedly and continuously expressed in the spermatogonial population, the male mouse become infertile because the spermatogonia remain in an undifferentiated state in the testis, in which a large number of NANOS2-positive spermatogonia occupy the periphery of the seminiferous tubules (23). In addition, FLAG-tagged NANOS2 also localizes to the P-bodies in the spermatogonia in the manner similar to endogenous Nanos2 (Fig. S8 *D–F*). We prepared testis extracts from this mouse and performed immunoprecipitations with anti-FLAG antibodies and control IgG, and then subjected these immunoprecipitates to in vitro deadenylase assay (21) (Fig. 4*A*). As shown in Fig. 4*B*, cleavage of the poly(A) RNA substrate occurred only with NANOS2 immunoprecipitates, which also contains the CNOT6L and CNOT7 catalytic components of the deadenylation complex (Fig. 4*C*). These results lead us to propose that NANOS2 promotes the degradation of NANOS2-interacting mRNAs through the deadenylase activity of the CCR4-NOT complex.

NANOS2 Interacts with Specific mRNAs and May Promote Their Degradation. Based on our working hypothesis, we further speculated that (*i*) the NANOS2 complex should contain specific mRNAs that would be degraded via NANOS2-mediated deadenylation, such that (*ii*) the expression levels of these transcripts would be low in wild-type male gonocytes but up-regulated in the absence of NANOS2. To test these possibilities, RNAs that coprecipitated with FLAG-tagged NANOS2 were purified and subjected to RT-PCR. Because we had previously shown that male gonocytes could enter meiosis in the absence of NANOS2, it was plausible that mRNAs involved in meiosis might be directly suppressed through NANOS2-mediated RNA degradation. As expected, *Sycp3*, *Stra8*, *Taf7l*, *Dazl*, and *Meisetz* (3, 24–27) transcripts that are implicated in meiosis were specifically detected only in the NANOS2 protein precipitates despite their very low expression in male gonads (Fig. 5 *A* and *B*). In contrast, the

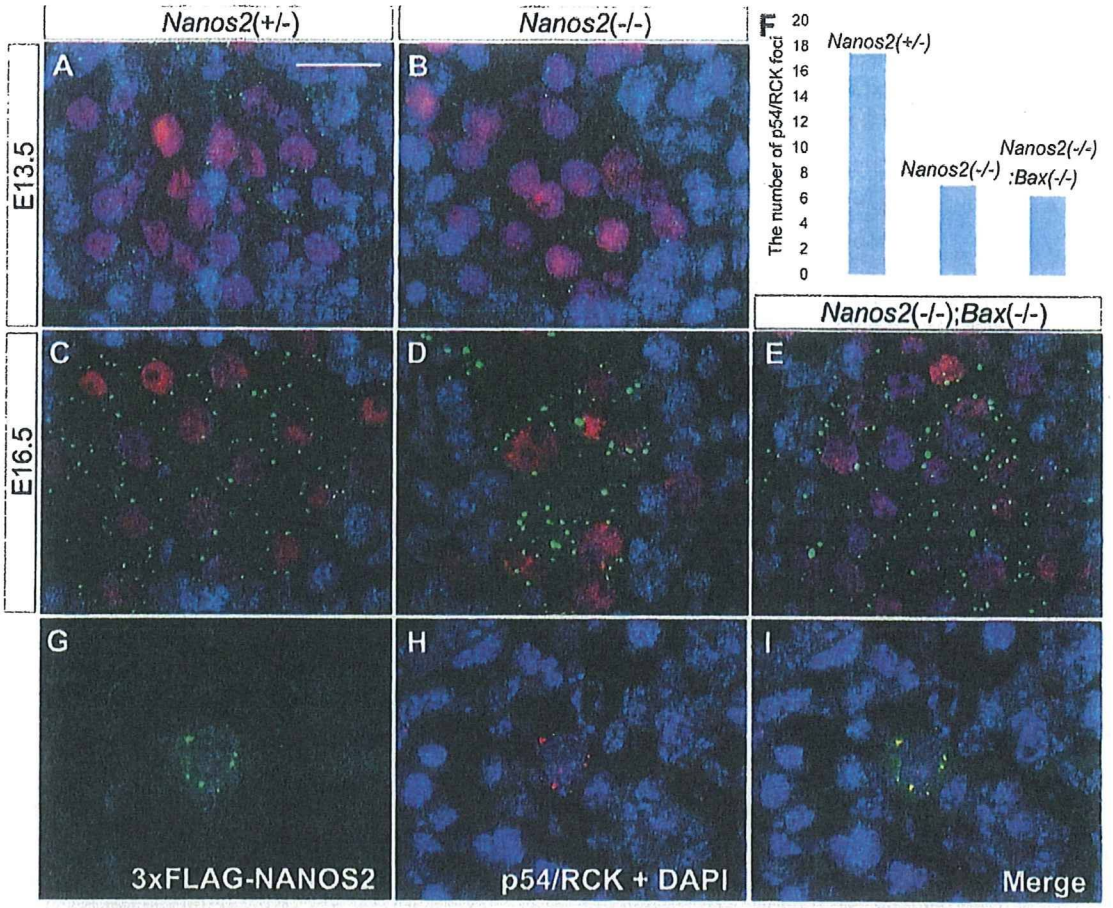

Fig. 2. Functional role of NANOS2 during the formation of the P-bodies. (*A–E*) Male gonadal sections from *Nanos2*$^{+/-}$ (*A* and *C*), *Nanos2*$^{-/-}$ (*B* and *D*), and *Nanos2*$^{-/-}$*Bax*$^{-/-}$ (*E*) embryos at stages E13.5 (*A* and *B*), and E16.5 (*C, D,* and *E*) were immunostained with p54/RCK (green) and TRA98 (red) antibodies. (*F*) Average number of p54/RCK foci per male gonocyte at E16.5 was quantified in each picture using ImageJ software (National Institutes of Health) and a cell counter, with the foci of less than a 20 permission value excluded using Photoshop (Adobe). The data shown correspond to two to three pictures. (*G–I*) A female gonadal section from a NANOS2-expressing embryo at E16.5 was immunostained with anti-FLAG (green) (*G*) and anti-p54/RCK (red) (*H*) antibodies. DNA was counterstained using DAPI (blue). (Scale bar in *A*, 20μm for *A–E* and *G–I*.)

G3pdh, *Dnmt3l* and *Dnmt3a* mRNAs did not show specific accumulation in the NANOS2 precipitates although they are all highly expressed in male gonads. These data indicate that the mRNAs involved in meiosis specifically interact with NANOS2 in vivo.

We next investigated global changes in gene expression upon the loss of *Nanos2* using comparative GeneChip analyses (Table S1). The resulting scatter plots showed that many genes become up- or down-regulated in *Nanos2*$^{-/-}$ male gonads by E15.5 (Fig. S9 *A–C*). For example, we found that the genes highly expressed only in male gonocytes, such as *Dnmt3l*, *Tdrd1* and *Miwi2/Piwi-like 4* (19, 28, 29), are down-regulated in the *Nanos2*$^{-/-}$ male gonads, whereas *Figla*, *Lhx8* and *Nobox*, which have been shown to be essential only for oogenesis and not for spermatogenesis (30–32), become accumulated in the *Nanos2*$^{-/-}$ male gonads (6) (Fig. S9 *D–I*). These results suggest that male gonocytes cannot enter the male pathways and become feminized by the up-regulation of female-type genes. In addition, and consistent with the results of our immunoprecipitation assay, *Sycp3*, *Stra8*, *Taf7l*, *Dazl,* and *Meisetzs* mRNAs were also found to be up-regulated in *Nanos2*$^{-/-}$ male gonads (Fig. 5 *C–G*). Our current findings thus indicate that NANOS2-interacting mRNAs become accumulated if NANOS2 is absent in male gonocytes, which in turn indicates that NANOS2 might be indirectly affecting the transcription of these genes, or that they are normally suppressed in wild-type male gonocytes through a NANOS2-directed mechanism, possibly a deadenylation pathway.

Discussion

Molecular Role of NANOS2. In our current study, we show that the CCR4-NOT deadenylation complex is coprecipitated with NANOS2 from male gonadal extracts. This is the first evidence that the interaction between a Nanos homolog and the CCR4-NOT deadenylation complex exists *in vivo,* although it has been shown using a yeast two-hybrid system that *Drosophila* Nanos can directly and potently bind to NOT4, a component of the CCR4-NOT complex (33). Hence, as suggested previously by Kadyrova et al. for *Drosophila* Nanos, and as confirmed by our present analyses in vivo, the recruitment of the CCR4-NOT deadenylation complex to target mRNAs may be a conserved function of the Nanos proteins.

We also found that NANOS2 localizes to P-bodies in the male gonocytes and adult mouse spermatogonia. P-bodies are known to be a central hub of RNA degradation, in which decapping enzymes and exonucleases are also localized. However, emerging evidence in other systems suggests that P-bodies not only function to degrade RNAs but also to store mRNAs in a translationally quiescent state until needed (13). In addition, *Drosophila* Nanos promotes the deadenylation of poly(A) tail in *hunchback* mRNA and represses its translation without changing the mRNA level

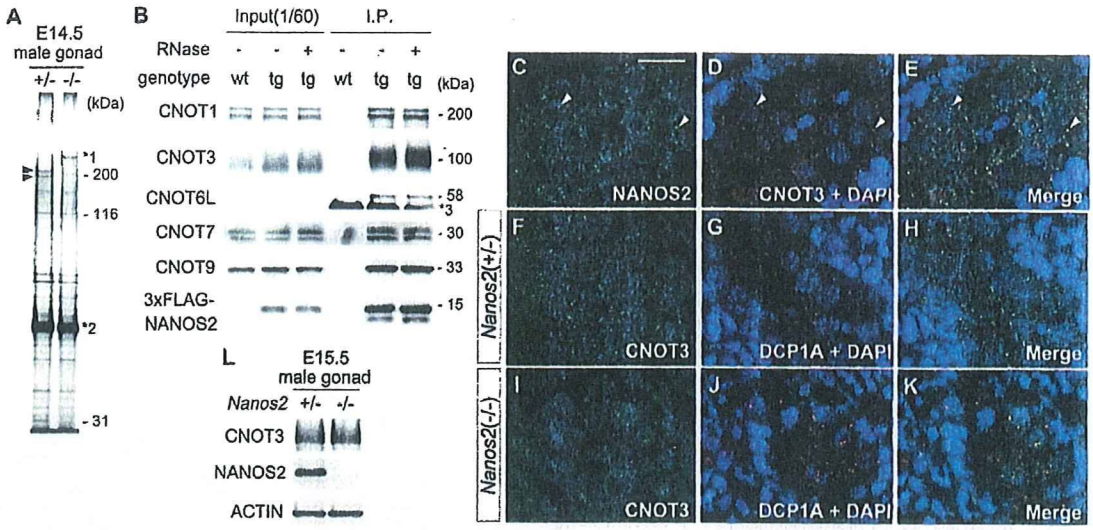

Fig. 3. Interaction between NANOS2 and the CCR4-NOT deadenylation complex. (*A*) Proteins coimmunoprecipitated with NANOS2 from E14.5 wild-type (lane 1) and *Nanos2*$^{-/-}$ (lane 2) male gonadal extracts using rabbit anti-NANOS2 antibodies. Arrowheads indicate CNOT1. *1, nonspecific band; *2, IgG polypeptide. (*B*) Immunoprecipitation–Western blot analyses of proteins from male gonadal extracts of wild-type and transgenic embryos expressing 3xFLAG-NANOS2. *3, IgG polypeptide from the anti-FLAG antibody. (*C–E*) Male gonadal sections from E15.5 embryos were immunostained with mouse NANOS2 (green) (*C*) and CNOT3 (red) (*D*) antibodies. Arrowheads in *C–E* indicate colocalization between NANOS2 and CNOT3. (*F–K*) Male gonadal sections from *Nanos2*$^{+/-}$ (*F–H*) and *Nanos2*$^{-/-}$ (*I–K*) embryos at E15.5 were immunostained with DCP1A (red) (*G* and *J*) and CNOT3 (green) (*F* and *I*) antibodies. DNA was labeled via DAPI counterstaining (blue). (*L*) Western blot analyses of proteins from the male gonads of *Nanos2*$^{+/-}$ and *Nanos2*$^{-/-}$ embryos at E15.5.

(34). We cannot therefore rule out the possibility that NANOS2 not only promotes the degradation of mRNAs involved in meiosis but also retains other transcripts at P-bodies to sequester them in a translationally inactive state during embryogenesis. These transcripts may be released from the P-bodies and translated to promote differentiation after birth as NANOS2 expression begins to disappear.

P-Body Formation in Male Mouse Gonocytes. P-bodies have been well characterized in yeast and mammalian cultured cells, and the in vivo status of these foci has begun to be described recently also in worms and flies (35–38). We found from our current analyses that P-bodies are specifically formed and/or maintained in the germ cells of male mouse embryonic gonads, whereas no such structures are detectable in somatic cells. Furthermore, female mouse gonocytes fail to maintain P-bodies at later stages of embryogenesis. We thus suggest that P-bodies play roles in cell-type specific differentiation during mouse development through RNA metabolism.

It has also been shown that P-bodies are dynamic structures and that their size and number reflects the status of the mRNA supply. If the transit of mRNAs into the P-bodies is inefficient, the size and number of these structures becomes extremely small. In contrast, they become larger when the mRNA decapping pathway is blocked (39, 40). Furthermore, it has been recently reported that deadenylation is required for P-body formation (41). Taking into account the data presented in these earlier reports and our current model, P-bodies would be expected to be small in *Nanos2*$^{-/-}$ male gonocytes because the mRNA supply to these structures and subsequent deadenylation efficiency would be inhibited in the absence of NANOS2. However, we were surprised to find that the sizes of the P-bodies

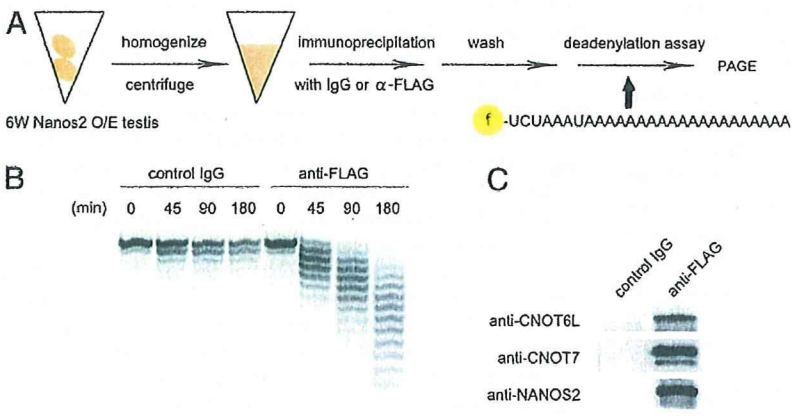

Fig. 4. The protein complex of NANOS2 and CCR4-NOT complex has in vitro deadenylase activity. (*A*) Schematic representation of the in vitro deadenylase assay method using NANOS2 over-expressing (O/E) testes. (*B*) FLAG-tagged NANOS2 was precipitated with anti-FLAG antibodies from the testis extracts of a 6-week-old NANOS2 O/E mouse and incubated with 5′-fluorescein isothiocyanate-labeled poly (A) RNA substrate for 0, 45, 90, and 180 min. Samples were then analyzed on a denaturing sequencing gel, as previously described (21) (*G*). (*C*) Western blot analyses reveaing that CNOT6L and CNOT7 are coprecipitated with FLAG-tagged NANOS2.

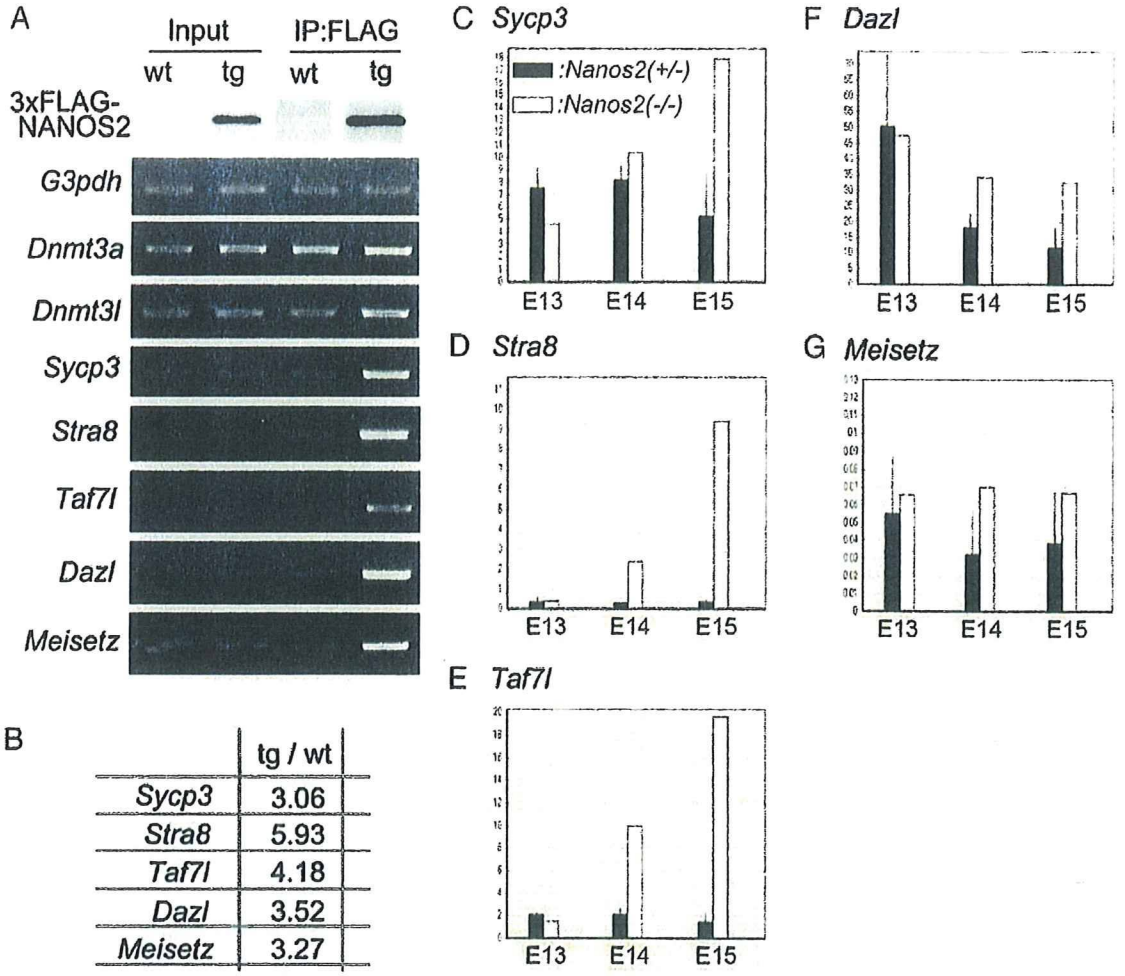

B

	tg / wt
Sycp3	3.06
Stra8	5.93
Taf7l	4.18
Dazl	3.52
Meisetz	3.27

Fig. 5. NANOS2 interacts with specific mRNAs and may promote their degradation. (*A*) Male gonadal extracts from wild-type (*wt*) and transgenic (*tg*) mice expressing FLAG-NANOS2 at E15.5 were subjected to immunoprecipitation (IP) with FLAG antibodies. RNA precipitates were analyzed by semi-quantitative RT-PCR. (*B*) Quantification of each mRNA enrichment from a FLAG IP of *tg* extracts using real-time RT-PCR. Fold enrichment of each mRNA coprecipitated from *tg* compared with those from *wt* is indicated. Mean value of three independent QRT-PCR results is shown. (*C–G*) Expression profiling of the *Sycp3* (*C*), *Stra8* (*D*), *Taf7l* (*E*), *Dazl* (*F*), and *Meisetz* (*G*) genes in male gonads from *Nanos2*$^{+/-}$ and *Nanos2*$^{-/-}$ embryos at E13.5-E15.5 using the Affymetrix GeneChip System as previously described (43) (*X*-axis; embryonic stage, *Y*-axis; expression level, black bars; *Nanos2*$^{+/-}$ embryos, white bars; *Nanos2*$^{-/-}$ embryos).

became larger in this biological context, although their number was decreased. These data thus indicate that male gonocytes have a unique program for P-body formation that occurs both in a NANOS2-dependent and -independent manner.

mRNAs Targeted by NANOS2. We elucidated that the protein complex of NANOS2 and CCR4-NOT complex has deadenylase activity in vitro. We thus expected that the poly(A) tail lengths of NANOS2-interacting mRNAs would be maintained without NANOS2. To test this scenario, we assayed the poly(A) tail length of NANOS2-interacting mRNAs. However, we could not observe clear shortening of the poly(A) tail in wild-type male gonads, possibly because of their low abundance. New experimental systems will be required in the future to address this issue.

On the other hand, it was noteworthy that we identified *Stra8* as a NANOS2-interacting mRNA because we have shown previously that *Stra8* is up-regulated at the transcriptional level in *Nanos2*$^{-/-}$ male gonocytes (6). These data together indicate that the suppression of *Stra8* in male gonocytes is ensured at both the transcriptional and translational levels, suggesting the critical functional importance of suppressing this gene during male gonocyte development.

Materials and Methods

Mice. Both the *Nanos2* and *Bax*-knockout mouse lines and PCR methods used for the verification of each mutant allele have been previously described (11, 42). The NANOS2-expressing mouse line has also been described (23) The transgene containing 3xFLAG-tagged *Nanos2* with the 3′-UTR under the control of Nanos2 enhancer (9.2 kb upstream sequence) was used for the production of the transgenic mouse line.

Histological Methods. For immunostaining, mouse gonads of both sexes were directly embedded in O.C.T. compound (Sakura) and frozen in liquid nitrogen. After sectioning (8 μm), samples were stained according to standard procedures.

Immunoprecipitation. Extracts of male gonads from E14.5 or E15.5 embryos were incubated with protein-A beads crosslinked with rabbit anti-NANOS2 antibody or anti-FLAG M2 affinity gel (Sigma).

In Vitro Deadenylase Assay. The testis extracts from NANOS2-expressing mice were incubated with anti-FLAG M2 affinity gel or Mouse IgG-agarose (Sigma). After several washes, precipitates were then subjected to a deadenylase assay as previously described (21).

RT-PCR. After synthesis of first-strand cDNAs with SuperScript III reverse transcriptase and $(dT)_{20}$ primer (Invitrogen), PCR analyses were carried out either using a regular or real-time protocol.

GeneChip Analysis. Total RNAs were purified from cells corresponding to the male gonads of *Nanos2-LacZ* knock-in heterozygous and homozygous embryos, and analyzed using a GeneChip Mouse Genome 430 2.0 Array (Affymetrix).

Details of the methods and primer sequences used for each section are provided in *SI Text*.

ACKNOWLEDGMENTS. We thank the following researchers for generously providing antibodies: Y. Nishimune (TRA98), S. Chuma and N. Nakatsuji (anti-TDRD1), T. Noce (anti-MVH), M. Kiledjian (anti-hDCP2), W. D. Heyer (anti-mXRN1), H. T. Timmers (anti-CNOT1), T. Tamura (anti-CNOT3), T. Yamamoto (anti-CNOT6L/Ccr4b), A. B. Shyu (anti-CNOT7/Caf1a), and H. Okayama (anti-CNOT9/Rcd1). We are also very grateful to M. Morita and T. Yamamoto for their technical advice and assistance with the *in vitro* deadenylase assay. We further thank Noriko Moriyama for technical assistance with the microarray experiments and Yuki Nakajima for help with the histological analyses. This work was partly supported by Grants-in-Aid for National BioResource Project and of the Genome Network Project of the Ministry of Education, Culture, Sports, Science and Technology, Japan.

1. Hayashi K, de Sousa Lopes SM, Surani MA (2007) Germ cell specification in mice. *Science* 316:394–396.
2. Bowles J, Koopman P (2007) Retinoic acid, meiosis and germ cell fate in mammals. *Development* 134:3401–3411.
3. Baltus AE, et al. (2006) In germ cells of mouse embryonic ovaries, the decision to enter meiosis precedes premeiotic DNA replication. *Nat Genet* 38:1430–1434.
4. Bowles J, et al. (2006) Retinoid signaling determines germ cell fate in mice. *Science* 312:596–600.
5. Koubova J, et al. (2006) Retinoic acid regulates sex-specific timing of meiotic initiation in mice. *Proc Natl Acad Sci USA* 103:2474–2479.
6. Suzuki A, Saga Y (2008) Nanos2 suppresses meiosis and promotes male germ cell differentiation. *Genes Dev* 22:430–435.
7. Kobayashi S, Yamada M, Asaoka M, Kitamura T (1996) Essential role of the posterior morphogen nanos for germline development in Drosophila. *Nature* 380:708–711.
8. Murata Y, Wharton RP (1995) Binding of pumilio to maternal hunchback mRNA is required for posterior patterning in Drosophila embryos. *Cell* 80:747–756.
9. Asaoka-Taguchi M, Yamada M, Nakamura A, Hanyu K, Kobayashi S (1999) Maternal Pumilio acts together with Nanos in germline development in Drosophila embryos. *Nat Cell Biol* 1:431–437.
10. Sato K, et al. (2007) Maternal Nanos represses hid/skl-dependent apoptosis to maintain the germ line in Drosophila embryos. *Proc Natl Acad Sci USA* 104:7455–7460.
11. Tsuda M, et al. (2003) Conserved role of nanos proteins in germ cell development. *Science* 301:1239–1241.
12. Suzuki H, Tsuda M, Kiso M, Saga Y (2008) Nanos3 maintains the germ cell lineage in the mouse by suppressing both Bax-dependent and -independent apoptotic pathways. *Dev Biol* 318:133–142.
13. Parker R, Sheth U (2007) P bodies and the control of mRNA translation and degradation. *Mol Cell* 25:635–646.
14. Eulalio A, Behm-Ansmant I, Izaurralde E (2007) P bodies: At the crossroads of post-transcriptional pathways. *Nat Rev Mol Cell Biol* 8:9–22.
15. Suzuki A, Tsuda M, Saga Y (2007) Functional redundancy among Nanos proteins and a distinct role of Nanos2 during male germ cell development. *Development* 134:77–83.
16. Hay B, Ackerman L, Barbel S, Jan LY, Jan YN (1988) Identification of a component of Drosophila polar granules. *Development* 103:625–640.
17. Bardsley A, McDonald K, Boswell RE (1993) Distribution of tudor protein in the Drosophila embryo suggests separation of functions based on site of localization. *Development* 119:207–219.
18. Toyooka Y, et al. (2000) Expression and intracellular localization of mouse Vasa-homologue protein during germ cell development. *Mech Dev* 93:139–149.
19. Chuma S, et al. (2003) Mouse Tudor Repeat-1 (MTR-1) is a novel component of chromatoid bodies/nuages in male germ cells and forms a complex with snRNPs. *Mech Dev* 120:979–990.
20. Kedersha N, Anderson P (2007) Mammalian stress granules and processing bodies. *Methods Enzymol* 431:61–81.
21. Morita M, et al. (2007) Depletion of mammalian CCR4b deadenylase triggers elevation of the p27Kip1 mRNA level and impairs cell growth. *Mol Cell Biol* 27: 4980–4990.
22. Meyer S, Temme C, Wahle E (2004) Messenger RNA turnover in eukaryotes: Pathways and enzymes. *Crit Rev Biochem Mol Biol* 39:197–216.
23. Sada A, Suzuki A, Suzuki H, Saga Y (2009) The RNA-binding protein NANOS2 is required to maintain murine spermatogonial stem cells. *Science* 325:1394–1398.
24. Yuan L, et al. (2000) The murine SCP3 gene is required for synaptonemal complex assembly, chromosome synapsis, and male fertility. *Mol Cell* 5:73–83.
25. Cheng Y, et al. (2007) Abnormal sperm in mice lacking the Taf7l gene. *Mol Cell Biol* 27:2582–2589.
26. Ruggiu M, et al. (1997) The mouse Dazla gene encodes a cytoplasmic protein essential for gametogenesis. *Nature* 389:73–77.
27. Hayashi K, Yoshida K, Matsui Y (2005) A histone H3 methyltransferase controls epigenetic events required for meiotic prophase. *Nature* 438:374–378.
28. Sakai Y, Suetake I, Shinozaki F, Yamashina S, Tajima S (2004) Co-expression of de novo DNA methyltransferases Dnmt3a2 and Dnmt3L in gonocytes of mouse embryos. *Gene Expr Patterns* 5:231–237.
29. Aravin AA, et al. (2008) A piRNA pathway primed by individual transposons is linked to de novo DNA methylation in mice. *Mol Cell* 31:785–799.
30. Soyal SM, Amleh A, Dean J (2000) FIGalpha, a germ cell-specific transcription factor required for ovarian follicle formation. *Development* 127:4645–4654.
31. Choi Y, Ballow DJ, Xin Y, Rajkovic A (2008) Lim homeobox gene, lhx8, is essential for mouse oocyte differentiation and survival. *Biol Reprod* 79:442–449.
32. Rajkovic A, Pangas SA, Ballow D, Suzumori N, Matzuk MM (2004) NOBOX deficiency disrupts early folliculogenesis and oocyte-specific gene expression. *Science* 305: 1157–1159.
33. Kadyrova LY, Habara Y, Lee TH, Wharton RP (2007) Translational control of maternal Cyclin B mRNA by Nanos in the Drosophila germline. *Development* 134:1519–1527.
34. Wreden C, Verrotti AC, Schisa JA, Lieberfarb ME, Strickland S (1997) Nanos and pumilio establish embryonic polarity in Drosophila by promoting posterior deadenylation of hunchback mRNA. *Development* 124:3015–3023.
35. Boag PR, Atalay A, Robida S, Reinke V, Blackwell TK (2008) Protection of specific maternal messenger RNAs by the P body protein CGH-1 (Dhh1/RCK) during Caenorhabditis elegans oogenesis. *J Cell Biol* 182:543–557.
36. Gallo CM, Munro E, Rasoloson D, Merritt C, Seydoux G (2008) Processing bodies and germ granules are distinct RNA granules that interact in C. elegans embryos. *Dev Biol* 323:76–87.
37. Noble SL, Allen BL, Goh LK, Nordick K, Evans TC (2008) Maternal mRNAs are regulated by diverse P body-related mRNP granules during early Caenorhabditis elegans development. *J Cell Biol* 182:559–572.
38. Lee L, Davies SE, Liu JL (2009) The spinal muscular atrophy protein SMN affects Drosophila germline nuclear organization through the U body-P body pathway. *Dev Biol* 332:142–155.
39. Sheth U, Parker R (2003) Decapping and decay of messenger RNA occur in cytoplasmic processing bodies. *Science* 300:805–808.
40. Eulalio A, Behm-Ansmant I, Schweizer D, Izaurralde E (2007) P-body formation is a consequence, not the cause, of RNA-mediated gene silencing. *Mol Cell Biol* 27: 3970–3981.
41. Zheng D, et al. (2008) Deadenylation is prerequisite for P-body formation and mRNA decay in mammalian cells. *J Cell Biol* 182:89–101.
42. Knudson CM, Tung KS, Tourtellotte WG, Brown GA, Korsmeyer SJ (1995) Bax-deficient mice with lymphoid hyperplasia and male germ cell death. *Science* 270: 96–99.
43. Kanno J, et al. (2006) "Per cell" normalization method for mRNA measurement by quantitative PCR and microarrays. *BMC Genomics* 7:64.

ENVIRONMETRICS
Environmetrics 2009; **20**: 1–13
Published online 8 May 2008 in Wiley InterScience
(www.interscience.wiley.com) DOI: 10.1002/env.898

An experimental design for judging synergism on consideration to endocrine disruptor animal experiments

Nobuhito Matsunaga[1*,†], Jun Kanno[2], Chikuma Hamada[3] and Isao Yoshimura[3]

[1]*Kyowa Pharmaceutical, Inc., 212 Carnegie Center, Suite 101, Princeton, NJ 08540, USA*
[2]*National Institute of Health Sciences, Tokyo, Japan*
[3]*Tokyo University of Science, Tokyo, Japan*

SUMMARY

This paper investigates an appropriate statistical design for an animal experiment to evaluate synergism of two test chemicals. It assumes a certain number of animals are divided into groups, each of which is treated with a combination of dose levels of two chemicals. A design is identified by the set of group size for each combination of doses, including the case where the dose of either one chemical is zero. The power of *t*-test to detect synergism by positive surplus of response on a simultaneous administration group from the additivity plane composed of the responses on single administration groups is adopted as the criterion for the appropriate design. The applicable design is investigated for the application to real cases of endocrine disrupter study conducted at the National Institute of Health Sciences of Japan.

It revealed that the dose level of the simultaneous administration group should be located inside or on the boundary of a triangular region and that the total number of animals should be the same as those for single administration groups. Copyright © 2008 John Wiley & Sons, Ltd.

KEY WORDS: additivity; animal experiment; experimental design; endocrine disruptor; synergism; triangular region

1. INTRODUCTION

In the past, environmental pollutants were regulated according to individual effects. However, recently, there has arisen the problems of combinations of complex pollutants, and regulations that address synergism have become necessary. As a result, experimental researches have been conducted on pollutant synergism. The investigation by Kanno, one of the authors (Kanno *et al.*, 2001) on the synergism of endocrine disruptors, using the rodent uterotrophic assay, is an example of such researches.

In our experiments using multiple test substances, dividing animals such as rats into multiple groups of single administration and simultaneous administration, we estimated the response when there is no synergism based on the response in the single administration group to investigate whether the response in the simultaneous administration group exceeds the estimated response.

*Correspondence to: N. Matsunaga, Kyowa Pharmaceutical, Inc., 212 Carnegie Center, Suite 101, Princeton, NJ 08540, USA.
†E-mail: matsunaga.nobuhito@kyowa-kpi.com

Received 21 February 2006
Accepted 20 October 2007

For the data analysis method used in this type of animal experiment to investigate synergism, Kelly and Rice (1990) proposed a method to evaluate the dose–response curve by smoothing method. Gennings and Carter (1995) and Gennings *et al.* (1997), on the other hand, proposed a method to evaluate synergism by using a model in which the response becomes flattened when there is no synergism. Using a similar plan to that of Gennings *et al.* (1997), Matsunaga *et al.* (2003) proposed a method to evaluate the difference in the responses with simultaneous administration of two substances from those estimated by applying an additive model to the data of single administration of each substance. They applied their proposed method to the actual data analysis. Other data analysis methods are also cited in Laska and Meisner (1989) and Machado and Robinson (1994).

For the experimental design evaluating the synergism, Hasegawa *et al.* (1996) proposed the experimental design of animal experiment for five or ten chemical mixture, and Straetemans *et al.* (2005) investigated a fixed-ratio design on *in vitro* study. Abdelbasit and Plackett (1982) and Tan *et al.* (2003) are also related to this issue. However, the situation of these researches differs from our case study. Our interest is limited to simply checking whether the effects of the chemicals are additive or not. And in the animal experiments, some assumptions and limitations are generated for the applicable information and experimental conditions.

In this kind of research, we thought that the problem of the experimental design is to determine appropriate dose levels for simultaneous administration and to select the appropriate number of animals for allocation to the dose levels. However, in the past research, the research directly related to this problem by the animal experiment was not found. Accordingly, based on the analysis methods proposed by Matsunaga *et al.* (2003), we investigated what type of design would be appropriate.

The paper is organized as follows. Section 2 introduces the conditions in the case study that motivated this paper, while Section 3 formulates the issues. Section 4 derived the appropriate design corresponding to the case studies dealt with this paper. Finally, Section 5 provides Conclusions and Discussions for future issues.

2. MOTIVATING CASE

According to the World Health Organization, an endocrine disruptor is defined as "an exogenous substance or mixture that alters function(s) of the endocrine system and causes adverse health effects in an intact organism, or its progeny or (sub)populations."

The effect of endocrine disruptors is not stimulated directly at the site of the adverse effect, but is mediated by the signal and occurs through nuclear receptor. Furthermore, there is more than one signal transduction system in humans and animals. Because nuclear receptors and transcription factors are redundant, there may be an interaction between different pathways, which leads to possible synergistic endocrine disruption action. Here the definition of "synergistic" is that if two chemicals produce the same endpoint, they bring about a larger response as compared to the anticipated response when these chemicals are purely added. Consequently, it is very important to realize the synergism between two endocrine disruptors such as "Genistein" and "bisphenol A (BPA)" through animal experiments for explaining the mechanism of action.

Both Genistein and BPA bind to estrogen receptors and elicit estrogenic responses to an organism including uterotrophic responses. Genistein is a phytoestrogen found relatively abundant in soybeans and its derivative foods. BPA is the basic monomer of polycarbonate plastic and epoxy resins widely used as a lining for food and beverage cans, in hard plastic baby and water bottles, toys, dental sealants, etc. It has been reported that BPA monomer can leached out to food and drinks especially when the

DOI: 10.1002/env

polymerization process is incomplete and/or the plastic is aged. These two estrogenic compounds can be found very commonly in our food environment. Therefore, it is of great importance from the point of the safety regulations to examine whether the combined effect is additive or synergistic.

For the experimental design of the research based on this background, some assumptions and limitations were generated for the applicable advanced information and experimental conditions. In the interests of simplicity, when explaining synergism research for two substances, the limitations are as follows.

First, before conducting the experiment that investigates synergism, advance knowledge can be obtained to some extent on dose–response curves for the single administration from preliminary experiments using each substance. Therefore, if the dose–response curve is nonlinear, by appropriate transformation of variables for the dose and response, it is possible to assume the dose–response curve to be approximately linear.

Second, the maximum dose of each substance used in the experiment is limited. We, for example, recognize in our experiments that the signal transduction system amplifies the signal at significantly smaller doses as compared to the dose used in normal toxicity studies. Other toxicities appear with higher doses, so that the endocrine disruption effect to be investigated is concealed. Because these maximum doses, $D_{A\max}$ and $D_{B\max}$, generally can be obtained through preliminary experiments, the range of dose levels used in the experiments can be limited.

Third, because various kinds of test substances are to be investigated, the number of animals, n, used in each experiment is relatively small. In our actual experience, the number of animals is approximately 40–50.

Fourth, the fundamental form of the experiment for investigating synergism is roughly decided. In an experiment using two substances A and B, we set single administration groups of G_{00} (at a dose level of 0), G_{A2}, and G_{B2} (at the maximum dose levels of $d_{A2} = D_{A\max}$ and $d_{B2} = D_{B\max}$, respectively), and groups G_{A1} and G_{B1} (at the middle dose levels of d_{A1} and d_{B1}, respectively), and administer the test substances after assigning the same number of animals n_s in every group. Independent of this, we set one or more simultaneous administration groups of G_{AB} with dose levels of the two substances at d_A and d_B. We measure responses by performing the experiment with this type of design, and estimate dose–response curves by forecasting synergism from the single administration group to confirm whether the response obtained in the simultaneous administration group is larger compared to that estimated.

Fifth, the observed response is usually quantitative variable such as the uterine weight of rats, which generally shows normal distribution, because it is difficult to define the additivity/synergism for the response in qualitative values.

Under the above conditions, what should be questioned for the design is what the most appropriate dose for simultaneous administration is, and whether to have more or less animals for the simultaneous administration group as compared to the single administration group. In order to obtain guidelines for these, this paper generalizes and formulates the above mentioned problems to make numerical evaluations under some conditions.

3. FORMULATION OF PROBLEM

3.1. Definition of synergism

In order to simplify the discussion, hereafter, we assume that there are two test substances denoted by A and B.

There have been many discussions in the past for how to define the terms additivity, synergism, and antagonism. Synergism is not defined unconditionally (Hewlett and Plackett, 1959; Berenberm, 1989).

DOI: 10.1002/env

Table 1. Difference between factorial design and triangular design

	Dose of A		
Dose of B	d_{A0}	d_{A1}	d_{A2}
(a) Factorial design			
d_{B0}	(1)	(2)	(3)
d_{B1}	(4)	(6)	(7)
d_{B2}	(5)	(8)	(9)
(b) Triangular design			
d_{B0}	(1)	(2)	(3)
d_{B1}	(4)	(6)	
d_{B2}	(5)		

Single chemical is administered at (1)–(5), whereas combination of two chemicals is administered at (6)–(9).

In fact, in the general remarks of these studies, many ideas are introduced for discussing synergism such as "independent joint action," "potentiation," "simple similar action," "complex action," and "dissimilar action." We will first explain the definition of synergism that is adopted in this paper.

From the standard statistical viewpoint, the dosages set certain dose level for the respective two substances as shown in Table 1(a). If the response at the simultaneous dose level is the sum of the effects generated by single substances, then the effect is considered to be additive. On the other hand, if it is large, there is a positive interaction and the effect is synergistic.

However, with toxic responses like endocrine disruption action, this point of view is not appropriate. Because, for this toxic response, as pointed out by, for example, Hasegawa *et al.* (1996), it is impossible to establish response linearity at doses that exceed the maximum dose for the respective substances, and thus it is impossible to determine whether a positive interaction is attributable to synergism or nonlinearity. Therefore, the following definition that expresses the tenets of Hewlett and Plackett (1959) by isobologram is adopted in this paper.

Label the expected response at dose d_A and d_B (doses for A and B) as $f(d_A, d_B)$. Also, label the single administration dose of A that results in an arbitrary response E as D_A, so that $f(D_A, 0) = E$. Similarly, label the dose of substance B that has expectation E as D_B. In the cases that motivated this study, A and B generate their responses in a similar stimulation process, the expected effects are proportional to the doses of A and B, and the effects of the two substances are additive. If these conditions hold, then $f(d_A, d_B) = E$ whenever (d_A, d_B) satisfies Equation (1).

$$\frac{d_A}{D_A} + \frac{d_B}{D_B} = 1 \tag{1}$$

The reason is that because a combination of dose levels like this represents simultaneous administration of A and B at an arbitrary ratio, using the amount that brings about a response of the same magnitude. If a response of magnitude E is consequently generated as expected, there is no special combined effect between the two chemicals. In this paper, when this relationship holds, the effect of the two substances is additive, or the two substances satisfy additivity.

On the other hand, if the two substances generate a synergistic response in different stimulation processes, it is considered that $f(d_A, d_B) > E$ is established with respect to an arbitrary (d_A, d_B) that satisfies Equation (1). In this paper, when this relationship is established, the two substances are synergistic, or satisfy synergism.

DOI: 10.1002/env

3.2. *Terminology, notation, and assumption*

The two-dimensional plane by plotting d_A (dose of A) on the x-axis and d_B (dose of B) on the y-axis is referred to as the dose plane, and the three-dimensional space by plotting the response on the z-axis above the dose plane is referred to as the response space.

In the experiment, the response is measured for each individual animal. The response that is measured is called the response variable, and is generally expressed by the symbol Z. The response variable Z measured for each individual is set as a random variable that follows a normal distribution independent of other individuals. Since it is assumed that the endpoint is organ weight as a target for application in the case study, such as endocrine disruptor study, it is considered that the assumption of the normal distribution is empirically valid. When the dose of the two substances administered is (d_A, d_B), the expected value is $E\{Z\} = f(d_A, d_B)$.

For single administration, that is, when the dose of one test substance is 0, Equation (2) can be assumed concerning the dose–response curve f.

$$f(d_A, 0) = \beta_0 + d_A\beta_A,\ f(0, d_B) = \beta_0 + d_B\beta_B \tag{2}$$

This assumes the dose–response curve for single administration to be linear. With this assumption, $f(d_A, d_B)$ is expressed by Equation (3). The two substances are additive if the hypothesis H_0 of Equation (4) holds, while synergistic if the hypothesis H_1 holds.

$$f(d_A, d_B) = \beta_0 + d_A\beta_A + d_B\beta_B + \Delta(d_A, d_B) \tag{3}$$

$$H_0 : \Delta(d_A, d_B) = 0,\ H_1 : \Delta(d_A, d_B) > 0 \text{ for all } (d_A, d_B) \tag{4}$$

The value of the dose used in the experiment is called the dose level, the collection of animals allocated for the dose level is called a group, and the number of animals for each group is called the group size, and the dose level of the group on the dose plane is called the group point. With this terminology, it is defined that "design is the set of group point and group size."

For numerical evaluation described in the next section, five groups of group size n_s for single administration and one group of group size n_m for simultaneous administration as described in Table 1(b) are assumed as the design. For the single administration group, the group points are set to be $(0, 0)$, $(d_{A1}, 0)$, $(d_{A2}, 0)$, $(0, d_{B1})$, $(0, d_{B2})$, and the response variables are distributed as normal with variance σ_s^2. For the simultaneous group, the group point is set to be (d_A, d_B), and the response variable is distributed as normal with variance σ_m^2

Let the sample mean of response variable in each group be Z_{00}, Z_{A1}, Z_{A2}, Z_{B1}, Z_{B2}, and Z_{AB}, respectively. It is assumed that $Z_{00}, \ldots, Z_{B2}$ are distributed as normal with the mean of Equation (2) and the variance σ_s^2/n_s, while Z_{AB} is distributed as normal with the mean of Equation (3) and the variance σ_m^2/n_m.

3.3. *Criterion for the appropriate design*

As criterion for the most appropriate design, it is natural to use the power in the hypothesis test of "H_0 versus H_1." Because the model is a linear model and the hypothesis is a linear hypothesis, a one-sided

DOI: 10.1002/env

t-test (or Welch test) with Equation (5) is naturally set as the test statistic.

$$T = \frac{\hat{\Delta}}{\sqrt{\hat{V}(\hat{\Delta})}} \tag{5}$$

Here, $\hat{\Delta}$ is the least square estimator of Δ, and the denominator of the statistics is the square root of the variance estimator.

The critical value of this test statistics is $t(\nu, \alpha)$, the upper 100α percentile of the t-distribution with degree of freedom ν, and the test is a one-sided test. In other words, A and B are judged to be synergistic when $T > t(\nu, \alpha)$.

This test, in short, detects the synergism when there is a statistically significant difference between Z_{AB} and the estimate obtained from the single administration groups assuming the dose–response surface under H_0.

4. EXAMPLES OF RECOMMENDED DESIGN

4.1. Real examples motivated the problem

We conducted many experiments and selected endocrine disruptor study as case study. This study was performed using triangular design such as Table 1(b). This design consisted of seven dose groups which included five group points for single administration and two group points for simultaneous administration. The endpoint was uterine weight gain and the main purpose was to evaluate whether the combined effect was synergistic or not. In order to explain the characteristic of the data, we took up two real examples. The details of these data are as follows.

Example 1. *Chemical A: genistein (mg/kg), chemical B: BPA (mg/kg)*

1. Group points for the single administration: $(d_A, d_B) = (0, 0), (12.5, 0), (25, 0), (0, 35), (0, 70)$.
2. Group points for simultaneous administration: $(d_A, d_B) = (6.25, 17.5), (12.5, 35)$.
3. Group size: $n_s = 6, n_m = 6, n = 42$.
4. Mean $\pm$ standard deviation of observed values

$$(d_A, d_B) = (0, 0) : 84.0 \pm 7.1$$

$$(d_A, d_B) = (12.5, 0) : 111.2 \pm 9.3, \quad (d_A, d_B) = (25, 0) : 149.5 \pm 33.7$$

$$(d_A, d_B) = (0, 35) : 138.4 \pm 16.2, \quad (d_A, d_B) = (0, 70) : 181.0 \pm 24.4$$

$$(d_A, d_B) = (6.25, 17.5) : 141.1 \pm 11.4, \quad (d_A, d_B) = (12.5, 35) : 180.2 \pm 26.8$$

5. Estimated value of Δ: 15.6.
6. Result of t-test: Significant in one-sided Welch test with significance level 2.5% $T = 2.19$, $\nu = 19$, $p = 0.02$.

Example 2. *Chemical A: diethylstilbestrol (μg/kg), chemical B: genistein (mg/kg)*

1. Group points for the single administration: $(d_A, d_B) = (0, 0), (0.1, 0), (0.2, 0), (0, 12.5), (0, 25)$.
2. Group points for simultaneous administration: $(d_A, d_B) = (0.05, 6.25), (0.1, 12.5)$.

DOI: 10.1002/env

3. Group size: $n_s = 6, n_m = 6, n = 42$.
4. Mean $\pm$ standard deviation of observed values

$$(d_A, d_B) = (0, 0) : 91.2 \pm 16.2$$
$$(d_A, d_B) = (0.1, 0) : 92.3 \pm 9.7, \quad (d_A, d_B) = (0.2, 0) : 96.5 \pm 5.4$$
$$(d_A, d_B) = (0, 12.5) : 165.4 \pm 27.0, \quad (d_A, d_B) = (0, 25) : 220.8 \pm 27.5$$
$$(d_A, d_B) = (0.05, 6.25) : 141.8 \pm 12.8, \quad (d_A, d_B) = (0.1, 12.5) : 183.5 \pm 10.3$$

5. Estimated value of Δ: 19.5.
6. Result of t-test: significant in one-sided Welch test with significance level 2.5% $T = 3.98$, $\nu = 31$, $p < 0.01$.

From the above results, we suggested that the combinations for these two agents were synergistic. The synergism was observed in the real situations such as endocrine disruptor study.

4.2. Recommended group point selection

The example introduced in the preceding section has two simultaneous administration groups. In this section, we investigate the most appropriate dose level among several dose levels in the case of one simultaneous administration group. The conditions in the investigation are as follows. The conditions are set pursuant to the example in the preceding section except for assuming $\sigma = 1$ without losing any generality.

4.2.1. Fixed condition.

1. Group points for single administration: $(d_A, d_B) = (0, 0), (1, 0), (2, 0), (0, 1), (0, 2)$.
2. Group size: $n_s = 6, n_m = 12$.
3. Parameters in the dose–response curve: $\beta_0 = 1.0, \beta_A = 1.0, \beta_B = 1.0$.
4. Variance σ^2: $\sigma_s^2 = \sigma_m^2 = 1.0$.
5. Nominal significance level of t-test: one-sided 2.5%.

4.2.2. Varied condition.

6. Group points for simultaneous administration: $d_A = 0.1(0.1)2.0, d_B = 0.1(0.1)2.0$.
7. Strength of synergism Δ:
   Case 1 (constant case): $\Delta = 1.0$
   Case 2 (square root case): $\Delta = 0.8\sqrt{(d_A + d_B)}$
   Case 3 (linear case): $\Delta = 0.6(d_A + d_B)$

Numerical calculations were performed to calculate the power under the above conditions. The left-hand side of Figures 1–3 shows a three-dimensional display on the vertical axis above the dose plane of the power in Cases 1–3, respectively. On the other hand, the right-hand side of Figures 1–3 represents power functions when $d_A = d_B$ at the dose level for simultaneous administration group.

DOI: 10.1002/env